Embry-Riddle Aeronautical University
SCHOLARLY COMMONS

International Journal of Aviation, Aeronautics, and Aerospace

Volume 8 | Issue 3 Article 8

2021

Performance of the EGNOS system in Algeria for single and dual frequency

Iahouaria Tabti
Algeria Space Agency, thouaria@yahoo.fr
Salem Kahlouche
skahlouche@cts.asal.dz
Belkacem Benadda
Abou Bekr Belkaid University of Tlemcen, Chetouan. Algeria., benadda.belkacem@gmail.com

Scholarly Commons Citation
Tabti, I., Kahlouche, S., & Benadda, B. (2021). Performance of the EGNOS system in Algeria for single and dual frequency. *International Journal of Aviation, Aeronautics, and Aerospace, 8*(3). Retrieved from https://commons.erau.edu/ijaaa/vol8/iss3/8

Introduction

Satellite-Based Augmentation Systems (SBAS) are used to enhance the accuracy and integrity of the existing GNSS system. This system uses a reference station covering a large area for gathering GNSS measurements and delivering correct data to users via geostationary satellites (Oday, 2011), with the objective to support requirements for civil aviation navigation from the en-route phase of flight to the vertically guided precision approach (Kaplan & Hegarty, 2006). SBAS system provides the following information in real time:

- Orbit and clock corrections of existing navigation satellites, and estimation of associated satellite errors or User Differential Ranging Error (UDRE)
- Correction and estimation of ionospheric error for a given grid points, known as Grid Ionospheric Vertical Error (GIVE)

Several SBAS are currently in service allowing civil aviation to operate across the world: WAAS in North America (United States and Canada) and EGNOS in European countries and MSAS in the Asia Pacific region. EGNOS is available for Safety-of-Life for aviation since March 2011 and for open service since October 2009. Currently, most commercial GPS receivers can use EGNOS signals, which allows the development of many applications and various types of experimentation (ESA, 2011). An extension of the EGNOS system for the Mediterranean (MEDA) is planning; this extension permits to improve simultaneously the performance of EGNOS and MEDA service area and at the same time open new application in developing countries (Lyon et al., 2006).

The terrestrial segment of EGNOS is composed of a 39 reference stations RIMS (Ranging & Integrity Monitoring Stations) located inside and outside Europe, presented in Figure 1 (ESSP, 2018); 2 control centers MCC (Mission Control Centers), and 6 uplink stations NLES (Navigation Land Earth Stations). The main function of RIMS station is to collect GPS data, monitor GPS satellites and send raw data to MCC.

Figure 1

Locations of EGNOS RIMS Stations

Initially, European Space Agency (ESA) proposed a site at Tamanrasset (southern Algeria) for the setting up of an EGNOS RIMS station in Algeria. However, this site was considered technically not very favorable for interference reasons (site survey); then, the ESA proposed to move this site to another site located between 30° and 35° of latitude. The preliminary results of the optimal choice and feasibility study for RIMS station in Algeria, shows that setting up a site in central Algeria (Ghardaïa City) would allow a better use of EGNOS system as well as the extension of its zone of coverage availability (Kahlouche & Tabti, 2015). The current SBAS signals are delivered on L1 frequency, and they have a structure identical to the GPS L1/CA signal. Future SBAS satellites will use L1 and L5 frequencies, the advantage of using two signals at two separate frequencies is that ionospheric correction can directly estimate and remove. A brief presentation of these two GPS L1 and L5 is given by:

- The L1 frequency is 1575.42 MHz, and the bandwidth is 20 MHz. It is modelled with a C/A and P(Y) codes. The civil C/A pseudo random noise (PRN) code has a 1.023 MHz chipping rate.
- The L5 frequency is 1176.45MHz, and the bandwidth is 24 MHz. It has I and Q codes. The civil PRN code on L5 has a 10.23 MHz chipping rate. This new L5 is more advance than existing L1 (Shau-Shiun, 2002).

Purpose

The purpose of this paper is to analysis the potential of the next generation of EGNOS V3 for civil aviation applications, and to show that the setting up of a RIMS station is also primordial even with EGNOS V3 using L1 and L5.

Satellite Based Augmentation System (SBAS) for Aviation

The SBAS systems can be used for aviation and terrestrial applications. SBAS for aviation is a safety critical service which providing regional augmentation certified by the International Civil Aviation Organization (ICAO). SBAS for terrestrial enables various applications based on differential corrections. The goal of the Federal Aviation Administration is to use GPS for improved service and reduced infrastructure costs for aerial navigation. To accomplish this, the performance required of GPS should be improved. The requirements of civil aviation were standardised by ICAO and are based on different values for a specific procedure of flight. Figure 2 represents the different phases of flight, which allow operations of navigation during the corresponding procedure for civil aviation (Ciollaro, 2008).

Figure 2

Procedures of Flight for Civil Aviation

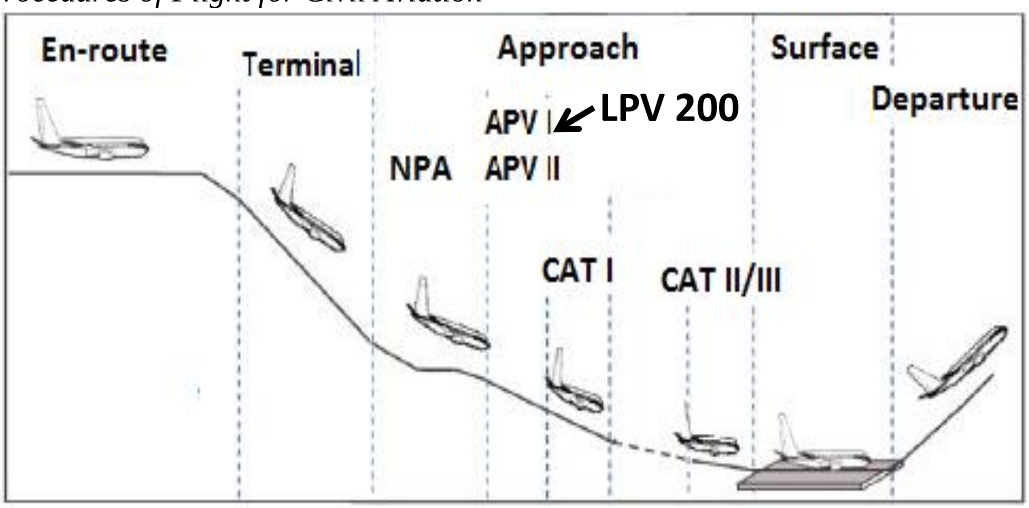

Researchers suggest that the requirements of CAT I may not be possible by SBAS in the near term (before deployment of GPS L5 frequency and Galileo constellation) (Kaleta, 2014; Shau-Shiun, 2002). A newer procedure has been added, called LPV 200 (lateral precision approach with vertical guidance), which provides the vertical guided approach capability to a height as low at 200 feet (61 meters). It is a type of operation that includes APV I and APV II (Speidel et al., 2013).

Protection Level Calculation

The receiver estimates in continuous time a position error, known as the protection level (PL), for each calculated position. The protection level is computed by using the UDRE, GIVE transmitted by SBAS system and other local error (Shuanggen, 2012). The horizontal and vertical protection levels (HPL/VPL) are compared with horizontal and vertical position error (PE) and a specified user level, called Alert Limit (AL) (Vassilev & Vassileva, 2010). When the protection level (PL) is superior to alert limit (AL), an alarm should be raised by the system, which is then declared unavailable to perform the intended critical operation (Simon et al., 2012). The horizontal and vertical protection levels are calculated as:

$$HPL = \mathrm{K_h} \times \mathrm{d_{maj}} \quad (1)$$

$$\mathrm{VPL} = \mathrm{K_v} \times \mathrm{d_U} \quad (2)$$

The parameters K_h and K_v are derive from the required level of performance and therefore depend on the application. In the case of precision approaches, the K values for HPL and VPL are $\mathrm{K_h}$ = 6.0 and $\mathrm{K_v}$ = 5.33:

- $d_u^2 = \sum_{i=1}^{n} S_{u,i}^2\, \sigma_i^2$ is the variance of model distribution that overbounds the true error distribution in the vertical axis. The parameter d_{maj} is obtained by the following expression (Grunwald et al., 2015) (RTCA, 2001) and $S_{u,i}$ is the partial derivative of position error in the vertical direction.

And $$\mathrm{d_{maj}} = \sqrt{\frac{\mathrm{d_{east}^2}+\mathrm{d_{north}^2}}{2} + \sqrt{\left(\frac{\mathrm{d_{east}^2}-\mathrm{d_{north}^2}}{2}\right)^2 + \mathrm{d_{EN}^2}}} \quad (3)$$

Where d_{east}^2 , d_{north}^2, and $\mathrm{d_U}$ are the East, North and Up (vertical) component variances of the position expressed in a Topocentric frame, $\mathrm{d_{EN}}$ represents the covariance of the East and North axis, they are calculated by (ESA, 2011):

- $d_{east}^2 = \sum_{i=1}^{n} S_{x,i}^2\, \sigma_i^2$ is the variance of model distribution that overbounds the true error distribution in the east axis and $S_{x,i}$ is the partial derivative of position error in the X direction and $S_{y,i}$ is the partial derivative of position error in the Y direction.
- $d_{north}^2 = \sum_{i=1}^{n} S_{y,i}^2\, \sigma_i^2$ is the variance of model distribution that overbounds the true error distribution in the north axis
- $d_{EN} = \sum_{i=1}^{n} S_{x,i}\, S_{y,i}\, \sigma_i^2$ is the covariance of model distribution in the east and north axis.

These parameters can be obtained from the variance/covariance matrix D, which is given by (Eurocontrol, 2003):

$$\mathrm{D} = \begin{bmatrix} \mathrm{d_{east}^2} & \mathrm{d_{EN}} & \mathrm{d_{EU}} & \mathrm{d_{Et}} \\ \mathrm{d_{EN}} & \mathrm{d_{north}^2} & \mathrm{d_{NU}} & \mathrm{d_{Nt}} \\ \mathrm{d_{EU}} & \mathrm{d_{NU}} & \mathrm{d_U^2} & \mathrm{d_{Ut}} \\ \mathrm{d_{Et}} & \mathrm{d_{Nt}} & \mathrm{d_{Ut}} & \mathrm{d_t^2} \end{bmatrix} = (\mathrm{G^T.W.G})^{-1} \quad (4)$$

Where the ith row of the geometry matrix G defined by:

$$G_i = [-\cos El_i \sin Az_i \quad -\cos El_i \cos Az_i \quad -\sin El_i \quad 1] \quad (5)$$

Where the positive azimuth Az_i defined clockwise from north, El_i is the satellite elevation and W is the weighting matrix of measurements defined as:

$$W = \begin{bmatrix} 1/\sigma_1^2 & 0 & \dots & 0 \\ 0 & 1/\sigma_2^2 & \dots & 0 \\ \vdots & \vdots & \dots & \vdots \\ 0 & 0 & \dots & 1/\sigma_N^2 \end{bmatrix} \qquad (6)$$

σ_i^2 represents the variance of residual error. It can be computed in single and dual frequency by equation 7 and 8. The computation of protection level for the different sources error is specified in the minimum operational performance standard (MOPS). Satellite error and ionospheric delay are corrected according to the MOPS standard. For local errors, such as tropospheric delay, receiver noise and multipath errors, they are corrected by using a standard model (RTCA, 2001).

Single-Frequency Protection Level Equation

For a single frequency, each measure contains four variances which are summed to provide the total variance. These terms are satellite clock, ephemeris corrections (σ_{flt}), ionospheric/tropospheric errors (σ_{UIRE} /σ_{trop}), and the airborne code noise/multipath error (σ_{air}). The total sigma confidence for a given satellite is calculated by (Walter et al., 2010).

$$\sigma_i^2 = \sigma_{i,flt}^2 + \sigma_{i,UIRE}^2 + \sigma_{i,air}^2 + \sigma_{i,tropo}^2 \qquad (7)$$

Where $\sigma_{i,flt}^2$, $\sigma_{i,UIRE}^2$, $\sigma_{i,air}^2$, and $\sigma_{i,tropo}^2$ are variance residuals of fast/long-term correction, variance of ionospheric/ tropospheric errors, and variance of airborne receiver error, respectively (Eurocontrol, 2003).

- The variance of fast and long-term corrections is defined in the SBAS MOPS as follows:

$$\sigma_{flt}^2 = \begin{cases} (\sigma_{UDRE}.\delta UDRE + \varepsilon_{fc} + \varepsilon_{rrc} + \varepsilon_{ltc} + \varepsilon_{er})^2, if \;\; RSS_{UDRE} = 0 \\ (\sigma_{UDRE}.\delta UDRE)^2 + \varepsilon_{fc}^2 + \varepsilon_{rrc}^2 + \varepsilon_{ltc}^2 + \varepsilon_{er}^2 \;\; if \;\; RSS_{UDRE} = 1 \end{cases} \qquad (8)$$

Where σ_{UDRE} is the model parameter from Message Type 2-6, 24, δUDRE is the user location factor in Message Type 27 and 28, otherwise $\delta UDRE = 1$, ε_{fc}, ε_{rrc}, ε_{ltc}, ε_{er} Fast correction degradation parameter, Range rate correction degradation parameter, and Long term correction degradation parameter respectively and RSS_{UDRE} is root-sum-square indicator in Message Type 10.

- The ionospheric residual error variance is determined using the following model:

$$\sigma_{i,UIRE}^2 = F_{PP}^2 \, \sigma_{UIVE}^2 \qquad (9)$$

$$F_{PP} = \left[1 - \left(\frac{R_e cos\theta_i}{R_e + h_I}\right)^2\right]^{-1/2} \quad (10)$$

Where R_e = 6378.137 Km (semi major radius of the earth), θ_i is the satellite elevation angle, h_I= 350 km (the maximum ionization height of the ionosphere), F_{PP} is the obliquity factor which relates the vertical ionosphere delay to the slant ionosphere delay along the line-of-sight vector, and σ^2_{UIVE} variance of interpolated user ionospheric vertical error.

- The model of the airborne receiver residual errors follows the MOPS formulation exactly, namely:

$$\sigma^2_{i,air} = \sigma^2_{i,noise} + \sigma^2_{i,multipath} \quad (11)$$

$\sigma^2_{i,noise}$ is the variance of receiver noise for a GNSS satellite and $\sigma^2_{i,multipath}$ is the variance of multipath error calculated by:

$$\sigma_{i,multipath} = 0.13 + 0.53.e^{-\theta_i/10\,deg} \quad (12)$$

With θ_i is elevation angle of the satellite (in degrees).

- Similarly for the residual tropospheric error, the MOPS models are adopted:

$$\sigma_{i,tropo} = \left(\sigma_{TVE}.\,m(\theta_i)\right) \quad (13)$$

$$m(\theta_i) = \frac{1.001}{\sqrt{0.002001 + \sin^2(\theta_i)}} \quad (14)$$

With σ_{TVE} is the variance of tropospheric vertical error. The fundamental steps for calculating vertical protection level using L1 frequency is doing by Figure 3.

Figure 3

The Protection Levels Calculation Ysing L1 (Shau-Shiun, 2002)

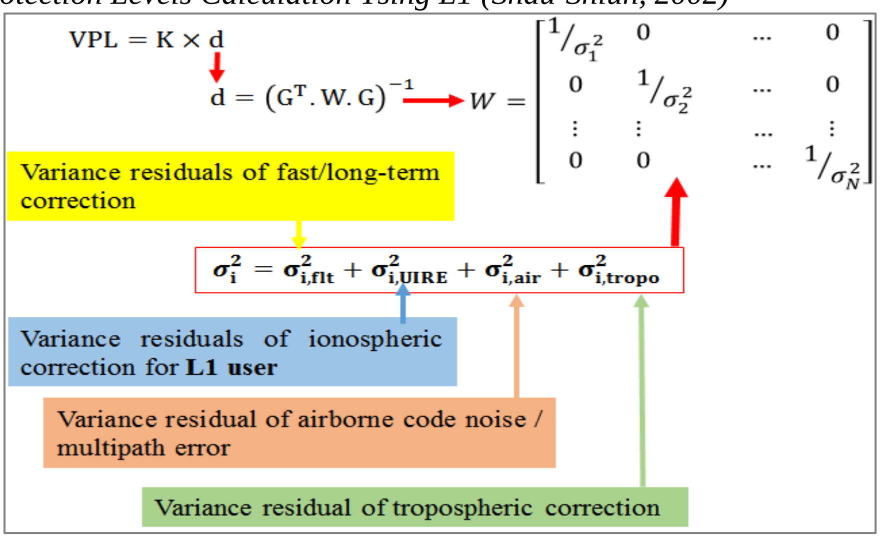

Dual-Frequency Protection Level Equation

The next GPS satellites will use a new civilian L5 signal; it should be in a protected aviation band. When the L5 frequency is combined with the L1, the ionospheric error can be estimated. The dual frequency variance for the corresponding satellite is defined by:

$$\sigma^2_{i,dual} = \sigma^2_{i,flt} + \sigma^2_{i,air,L1/L5} + \sigma^2_{i,trop} \tag{15}$$

Where $\sigma^2_{i,flt}$ and $\sigma^2_{i,trop}$ are defined in the same manner as in Equation (7), and $\sigma^2_{i,air,L1-L5}$ is the variance of L1/L5 dual-frequency airborne receiver error. The calculation of $\sigma^2_{i,air,L1/L5}$ considers the L1/L5 dual-frequency ionosphere error (Shau-Shiun, 2010). The fundamental steps for calculating vertical protection level using L1/L5 frequency is shown in Figure 4 (Shau-Shiun, 2002).

Figure 4

The Protection Levels Calculation Using L1/L5 Frequency

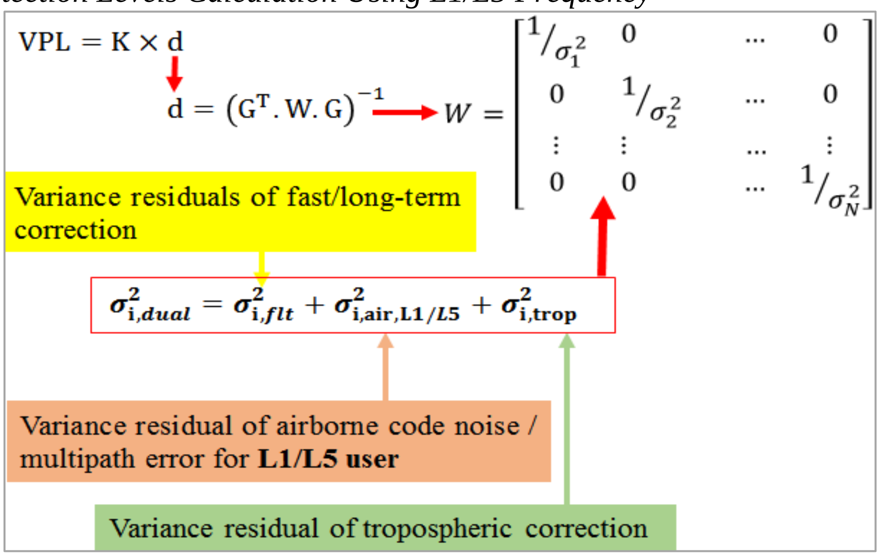

Methodology

The main contributor of SBAS performance comes from civil aviation safety requirements and they are different for each procedure. To analyses the availability and continuity, we used the open software SBAS Simulator 2 of the European Space Agency (ESA). The upgrade of SBAS Simulator is a software tool for analysing SBAS system performance. Simulations run in single and dual frequency (L1 and L1/L5) to study the impact of future SBAS evolutions. This tool can use almanac data to calculate the satellite's position for each epoch (ESA, 2015). The broadcast almanac used in this study corresponds to January 10, 2016, when there were 31 healthy satellites. The results depend on the choice of several parameters (RIMS filter, RIMS network…) and initial conditions (constellation, date, area, elevation mask ...); in this study, we considered the following parameters:

- Study area chosen: λ (longitude) ϵ [-30°, 40°]; φ (latitude) ϵ [15°, 55°] (to permit the complete coverage on Algeria) and the RIMS reference stations used in this study are composed of 39 existing operational stations.
- In single frequency, the ionospheric model used is based on an interpolation depending on existing RIMS stations. Otherwise, for L1/L5 frequency, ionospheric error can estimate.
- UDRE = 1, $\sigma_{i,noise}$= 0.36 m and $\varepsilon_{fc} = \varepsilon_{rrc} = \varepsilon_{ltc} = \varepsilon_{er} = 0.0$ and protection level (PL) is calculated each 10 minutes with an Alert Limit (AL) shown in table 1 (Ciollaro, 2008).

Table 1

Horizontal and Vertical Alarms Limits in Meters, for APV I, LPV 200, APV II, and CAT I

	APV I	LPV 200	APV II	CAT I
HAL(m)	40	40	40	40
VAL(m)	50	35	20	15

The four procedures are different in vertical alarm limits; therefore, for horizontal availability and continuity, one simulation will perform.

EGNOS Availability Simulation Analysis

Availability is an indication of the ability of the system to provide usable service within the specified coverage area. EGNOS availability is measured by the percentage of time in which the protection levels (HPL and VPL) are below their defined limits HAL and VAL as set in table 1, EGNOS is available at a certain epoch when calculated protection levels are less than the alarm limit as HPL < HAL and VPL < VAL (Simon, 2012).

The HPL and VPL are calculated at a 5-degree grid spacing to determine if EGNOS for each procedure is available at each of these grid points. Adding up the availability of each grid point over a 24-hours period in a region determines the availability of EGNOS. Figure 5 provides performance for L1 frequency, the brown zone is the area in which the system is available at more than 90% (HPL < HAL= 40 meters).

Figure 5

EGNOS Horizontal Availability Using L1 Frequency for all Procedures with Operational RIMS Network

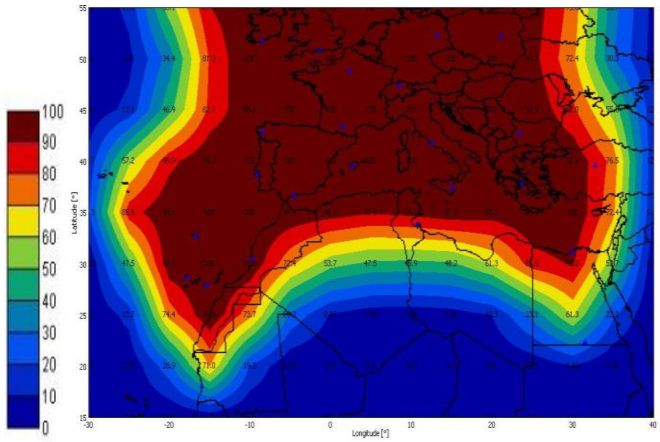

As shown in Figure 5, horizontal availability using single-frequency L1 is better in northern Algeria for latitude φ >35°. EGNOS provides more than 90% availability; this availability is assured by the European and neighboring country stations, but these improvements are unable to push availability much beyond. The unavailability of the system is explained by the limits of RIMS station.

Thus, the only option to expand the availability in Algeria for L1 frequency is to add RIMS station in the country (Tabti et al., 2018)**.** However, in EGNOS V3 using dual frequency (L1/L5), results indicate that the horizontal availability is more than the 99% of HAL = 40 m on Algeria (required for all horizontal procedures). Figure 6 shows the histogram of EGNOS vertical availability and comparison between single L1 and dual frequency L1/L5 for all procedures.

Figure 6

EGNOS Vertical Availability (%) Using Single and Dual Frequency for all Procedures on January 10, 2016, with Operational RIMS Network

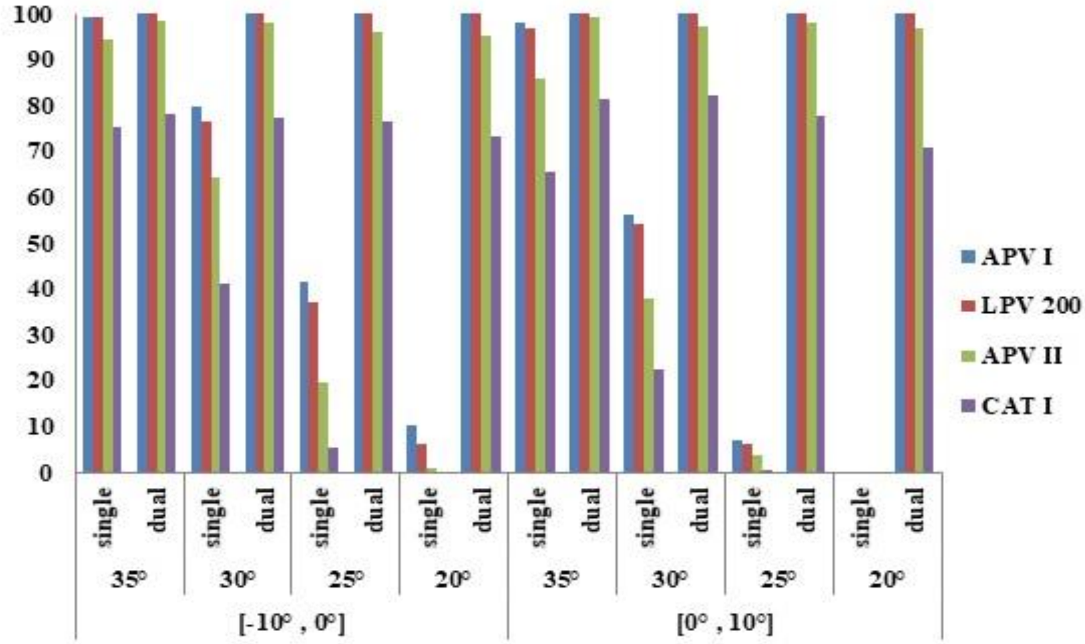

It can be observed that the availability of the new generation of EGNOS V3 using L1/L5 is better than EGNOS V2, which uses L1 only for all procedures. Coverage is slightly improving with L1/L5 frequency; it provides greater availability. This availability is not driven by ionospheric corrections, consequently the availability can be extended to places outside areas with dense reference ground stations of the network. Simulation results for the single-frequency show that the vertical availability of APV I and LPV 200 for latitude $\phi > 30°$ is more than 54%, this percentage is decreased for APV II and CAT I. Adding a new RIMS station in Algeria can improve vertical availability slightly for all procedure (Kahlouche & Tabti, 2015).

However, in dual frequency, the simulation results show that the vertical availability can reach 100% for APV I and LPV 200, and 99.13 % for APV II, while for CAT I, the availability is between 70.86 % and 82.24 %. The EGNOS system would not obviously achieve more than 99 % of the APV II and CAT I vertical availability VAL = 20 meters and VAL = 15 meters respectively. To complete 99.99% vertical availability, additional RIMS station in Algeria is required also with the use of two frequencies. Table 2 presents the availability obtained by EGNOS V2 using L1 frequency, which Algerian reference station is used for simulation (site at Ghardaïa, which geographic coordinates are 32° 22′ 54″ N, 3°

47′ 58″ E). The site considered for the analysis is chosen with the intention to compare the availability of EGNOS in Algeria.

Table 2

Availability Coverage for all Procedures of Flight Using L1 Frequency

Procedures of flight	ϕ : Latitude λ : Longitude	25° [0° 5°]	30° [0° 5°]	35° [0° 5°]
APV I (HAL=40, VAL=50)	39 stations	3.45	49.30	92.70
	39 stations + Ghardaïa	24.75	81.35	100
LPV 200 (HAL=40, VAL=50)	39 stations	4.14	50.30	93.30
	39 stations + Ghardaïa	27.55	81.70	100
APV II (HAL=40, VAL=50)	39 stations	2.79	37.85	83.45
	39 stations + Ghardaïa	14.80	66.15	98.60
CAT I (HAL=40, VAL=50)	39 stations	0.48	23.75	63.05
	39 stations + Ghardaïa	7.25	45.85	81.30

Table 2 presents the improved availability by adding a Ghardaïa RIMS station to the existing reference station network using a single-frequency L1. Result simulation shows that the introduction of a new RIMS station, contribute greatly to the improvement of the availability in northern Algeria; the coverage area extends to the latitude superior to 30°, for APV I and LPV 200, however, there are some regions do not meet the APV II and CAT I requirement. Availability of the EGNOS system may be reduced due to the lack of raw satellite measurements; on the edge of RIMS network, some of satellites visible for users probably are not monitored by RIMS network. As a result, EGNOS signals broadcast by the geostationary satellites do not contain the data regarding these satellites.

Figure 7 shows the APV I simulation including and excluding RIMS stations in Algeria (site in Ghardaïa).

Figure 7

EGNOS Combined Availability for APV I Without a Station in Algeria (a) and With a Station in Algeria (b) Using L1 frequency on January 10, 2016

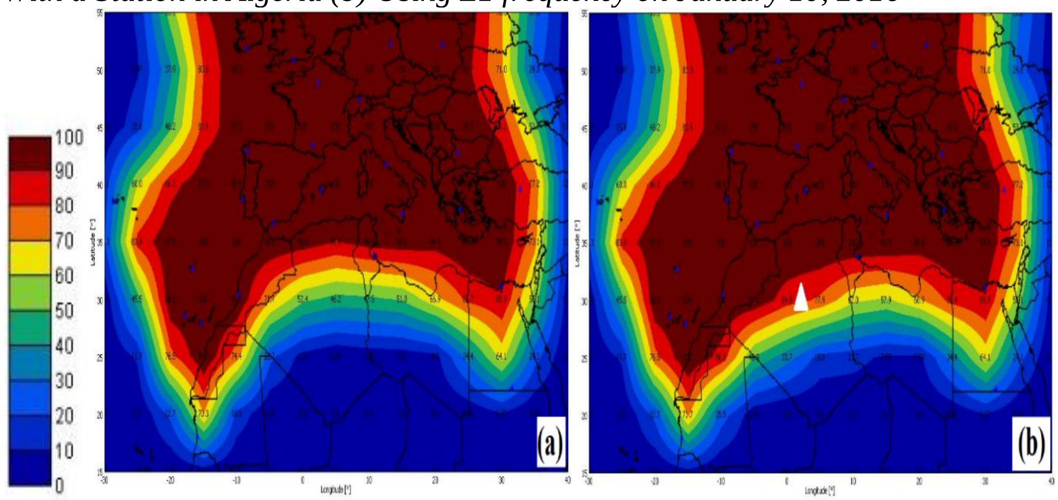

Figure 7 (a) shows that in Algeria, the availability is not assured for the users, in particular for latitude less than 30°. To investigate the consistency of the simulation results, we analyse the availability of EGNOS single frequency using real data collected at two sites located at 34° and 29° of latitude, on august 31 and 27, 2016, respectively. The protection level is calculated by gLAB software (Sanz et al., 2012). Figures 8 and 9 present the results of horizontal and vertical real availability of these sites, where no RIMS station was added.

Figure 8

Real Performance Availability Analysis: Horizontal Position Error HPE (blue), Horizontal Protection Level HPL (green), and Horizontal Alarm Limit HAL (red) at Each Site: (a) Site Located at 34° and (b) Site Located at 29° of Latitude

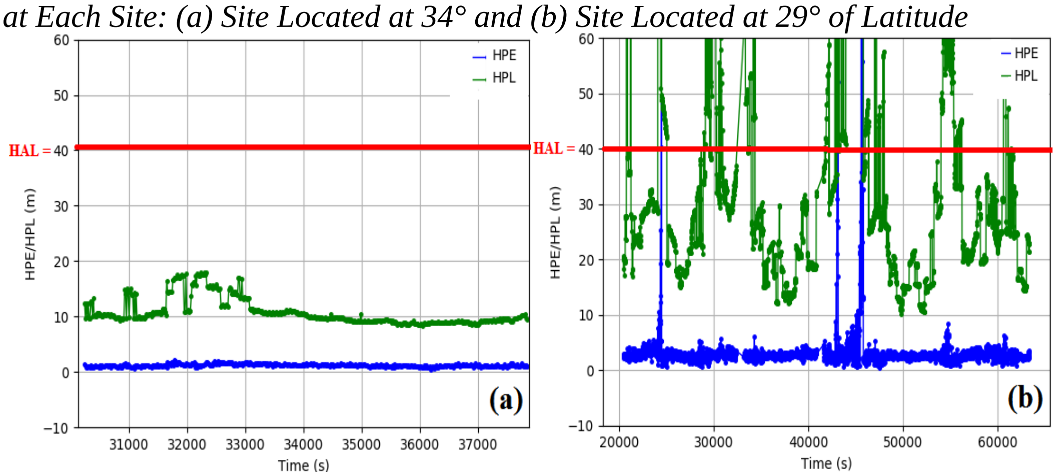

Figure 9

Real Performance Availability Analysis: Vertical Position Error VPE (blue), Vertical Protection Level VPL (green), and Vertical Alarm Limit VAL (red) at Each Site: (a) Site Located at 34° and (b) Site Located at 29° of Latitude

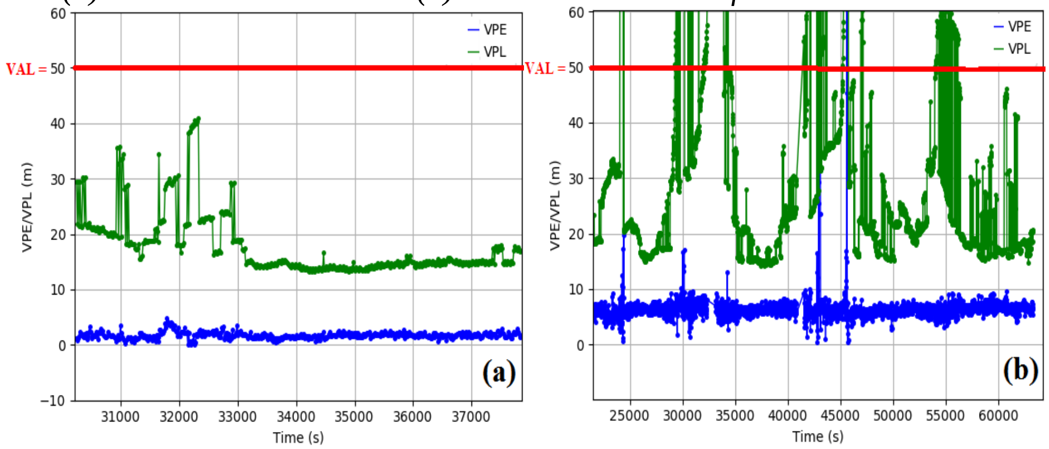

For a site located at 34° of latitude, the horizontal and vertical protection level are always lower than the horizontal and vertical alarm limits (HAL=40 m and VAL=50 m), which means that EGNOS is available for the entire time of observation. It is also demonstrated that horizontal and vertical positioning errors of GPS corrected by EGNOS for a site located at latitude superior to 32° are better than GPS only (Tabti et al., 2020).

However, for a site located at 29°, the horizontal and vertical protection levels are not always below the alarm limit (HAL= 40 m and VAL= 50 m) during the observation period. Therefore, the availability is not guaranteed for the entire period of observation and the requirements of the APV I approach cannot be reached. The results can be improved if a RIMS station will be set up in the country as shown on the simulation results in Figure 7 (b).

EGNOS Continuity Simulation Analysis

The continuity is the ability of the system to perform its operation without unscheduled interruptions along the planned operation. From the definition of continuity, after the availability at each moment knows, the simulator first computes the number of discontinuity events (anomaly). Discontinuity events are observed at each time, when at epoch T_0 (PL < AL) then at epoch T_{0+16} (PL ≥ AL) (ESA, 2015). After the number of discontinuity events is known, the continuity risk is computed**.** The continuity risk is the probability that a procedure will interrupt; it is calculated by dividing the total number of continuity events (PL>AL) within a time of [T0, T0+16 seconds] by the number of samples with valid and available navigation solution (Simon, 2012). Tables 3 provide a summary of the horizontal continuity events for all procedures.

Table 3

EGNOS Horizontal Discontinuity Events on January 10, 2016, with Operational RIMS Network

Longitude : λ	**[-10°,0°]**				**[0°,10°]**			
Latitude : φ	35°	30°	25°	20°	35°	30°	25°	20°
L1	45	61.66	-	-	56	67	-	-
L1/L5	0	0	-	-	0	0	-	-

The simulation results show that horizontal discontinuity events using single-frequency L1 (EGNOS V1) for all procedures are less than 56 at 35° in latitude. However, these discontinuity events are less than 61.66 in latitude 30°. This situation changes completely in dual frequency using L1/L5 (EGNOS V3); the discontinuity events are zero; consequently, the risks of continuity become zero. For EGNOS vertical discontinuity events, simulation used single and dual frequency is shown in figure 10.

Figure 10

EGNOS Vertical Discontinuity Events for all Procedures on January 10, 2016, with Operational RIMS Network

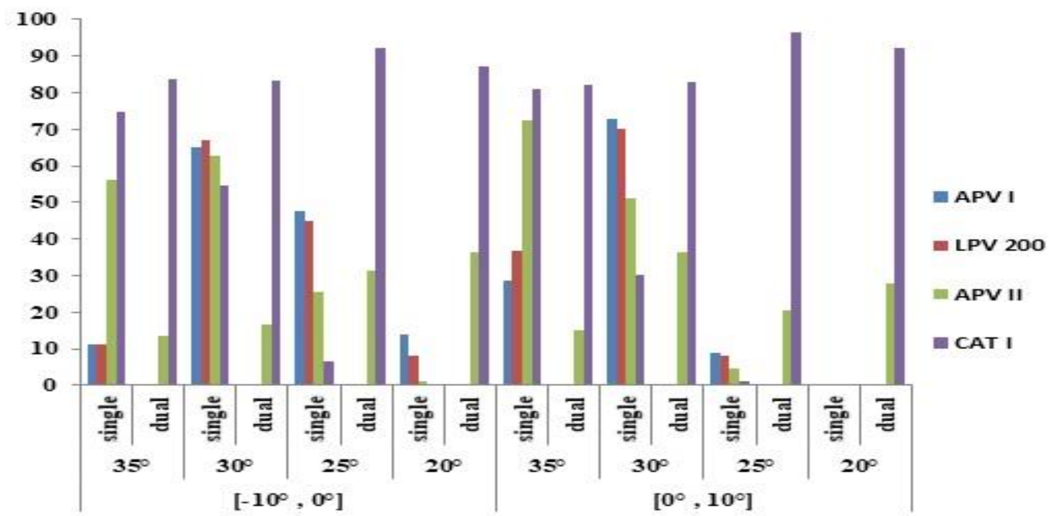

According to Figure 10, vertical discontinuity events for single-frequency L1 are greater than the dual frequency L1/L5 for all procedures. While for APV II and CAT I, in latitude 20° and 25°, the vertical discontinuity events for single frequency is inferior to the L1/L5 frequency; this is explained by the decrease of the alarm limit which is equal to 20 m and 15 m. Table 4 represents simulation of continuity risk using L1 frequency, excluding and including new RIMS stations in Algeria (site in Ghardaïa) for each procedure APV I, LPV 200, APV II, and CAT I.

Table 4

Continuity Risk for all Procedure on January 10, 2016 (39 Stations and 39 Stations + Ghardaïa)

Procedures of flight	ϕ : Latitude λ : Longitude	25° [0° 5°]	30° [0° 5°]	35° [0° 5°]
APV I (HAL=40, VAL=50)	39 stations	1	0.99	0.38
	39 stations + Ghardaïa	1	0.90	0
LPV 200 (HAL=40, VAL=50)	39 stations	1	0.99	0.6
	39 stations + Ghardaïa	1	0.90	0
APV II (HAL=40, VAL=15)	39 stations	1	1	0.75
	39 stations + Ghardaïa	1	0.97	0.13
CAT I (HAL=40, VAL=50)	39 stations	-	1	0.88
	39 stations + Ghardaïa	-	1	0.76

It is hereby possible to compare the EGNOS continuity with and without the new RIMS under the exact same conditions. The area with good continuity risk (close to 0) is extended to northern Algeria by adding station. The risk of continuity at 25 degrees and 30 degrees of latitude is always important for all phases of flight; to reduce this risk, the addition of a RIMS station in central of Algeria would be required.

The results show that when introducing the site in Ghardaïa, improvements in EGNOS continuity are seeing, particularly in the area between 30° and 35° in latitude, excepted for CAT I. For illustration purposes, the following figure (Figure 11) illustrates simulate APV I risk of continuity including and excluding RIMS stations in Algeria (site in Ghardaïa).

Figure 11

APV I risk of Continuity Without a Station in Algeria (a) and With a Station in Algeria (b) Using L1 Frequency on January 10, 2016

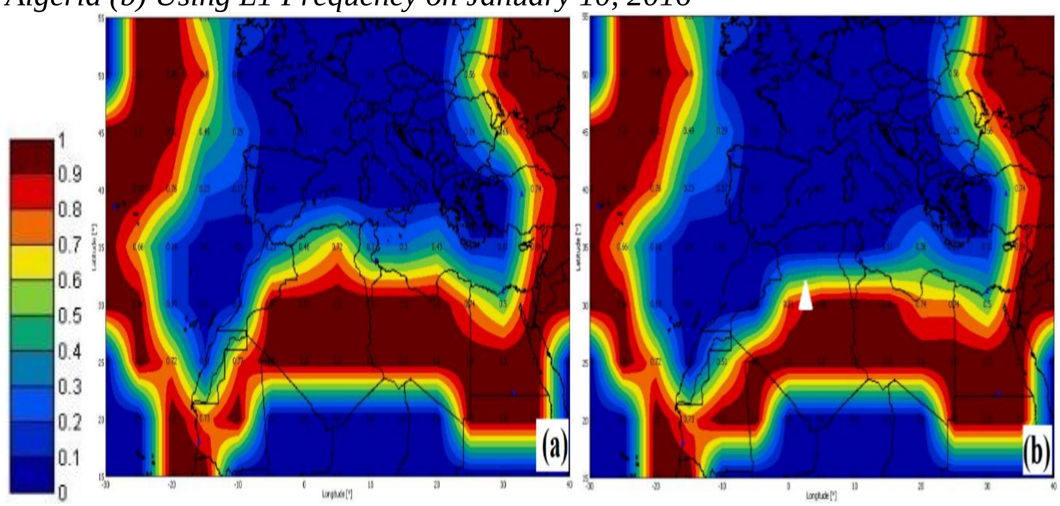

Conclusion

Currently, EGNOS covers most of Europe, with different coverage areas depending on the procedure of flight. The objective of this paper is to analyses the potential of the next generation of the EGNOS V3 for civil aviation applications in Algeria. In this work, APV I, LPV 200, APV II and CAT I procedures are studied. The paper showed that the availability and continuity obtained with EGNOS V2 and V3 are reduced for flight procedures associated with smaller alert limits. The main conclusions from the analyses performed are:

- EGNOS performance differs in various locations and may be degraded in the areas located at the edge of the nominal system coverage; then results confirmed that for L1 frequency (EGNOS V2), the coverage is in areas proximate to the European RIMS station network of EGNOS.
- The use of L1/L5 permit to extend the coverage in Algerian, and also permits the service to extend outside of the core network areas.
- Performance with two signals L1/L5 increase availability and continuity.
- The preliminary results of this paper show that availability of the EGNOS system in Algeria is improved by using L1/L5 for APV I and LPV 200. For APV II and CAT I.
- Adding a station in Algeria improves certainly the geographical distribution of RIMS stations in the West Mediterranean area. Finally, implementing for an EGNOS RIMS station in Algeria, and an optimal choice of the site, will certainly offer several advantages, mainly in terms of availability and continuity.

Acronyms

APV	Approach with Vertical Guidance
CAT I	Category 1
EGNOS	European Geostationary Navigation Overlay Service
GNSS	Global Navigation Satellite System
LPV 200	Localizer Performance with Vertical guidance at 200 feet
RIMS	Ranging and Integrity Monitoring Station
SBAS	Satellite Based Augmentation Systems
XAL	Horizontal or Vertical Alarm Limit
XPL	Horizontal or Vertical Protection Level

Acknowledgements

We greatly appreciate the help of Mr. M.R. BENHAMOU of the Algerian Society of Geophysics (ENAGEO) for the support provided.

References

Ciollaro, M. (2008). *GNSS multi system integrity for precision approaches in civil aviation*. Doctoral thesis, University of Naples "Federico II"- Italy.

ESA. (2011). *User guide for EGNOS application developers. ED 2.0*. Luxembourg: European Commission.

ESA. (2015). SBAS-SIM manual, upgrade of SBAS simulator. *Iguassu Software Systems, 1*(2).

ESSP. (2018). *Monthly performance report January*. https://egnos-user-support.essp

Eurocontrol. (2003). Technical notes on nSBAS; DocNo: PEG-TN-SBAS, issue: I. *Project: PEGASUS, 15*, 20-21.

Grunwald, G., Bakuła, M., Ciecko, A., & Kazmierczak, R. (2015). Examination of GPS/EGNOS integrity in north-eastern Poland. *IET Radar, Sonar & Navigation*. doi:10.1049/iet-rsn.2015.0053

Kahlouche, S., & Tabti, L. (2015). *Feasibility study and site choice for an EGNOS station in Algeria.* International Committee on Global Navigation Satellite Systems; Vienna. http://www.unoosa.org/pdf/icg/2015/presentations/06.pdf

Kaleta, W. Z. (2014). EGNOS based APV procedures development possibilities in the south-eastern part of Poland. *Annual of Navigation, 21*(1), 85-94.

Kaplan, E. D., & Hegarty, C. J. (2006). *Understanding GPS principles and applications* (2nd ed.). Artech house.

Lyon, A. W., Guida, U., Fernandez, J. L., & Perrin, O. (2006). *EGNOS: A step closer to operational qualification.* Proceedings of the 19th International Technical Meeting of the Satellite Division of the Institute of Navigation.

Oday, H. (2011). *WAAS integrity investigation for Canadian latitudes*. Doctorate thesis. University of Calgary.

RTCA. (2001). *Minimum operational performance standards for global positioning system/wide area augmentation system airborne equipment*. Washington, DC 20036. Supersedes DO-229B.

Sanz, J., Rovira-Garcia, A., Hernández-Pajares, M., Juan, M., Ventura-Traveset, J., López-Echazarreta, C., & Hein, G. (2012). *The ESA/UPC GNSS-Lab tool (gLAB): An advanced educational and professional package for GNSS data processing and analysis*. Proceedings of 4th International Conference on Space Applications Toulouse Space Show, France.

Shau-Shiun, J. (2002). *Analysis of a three-frequency GPS/WAAS receiver to land an airplane*. Proceedings of the 15th International Technical Meeting of the Satellite Division of the Institute of Navigation (ION GPS 2002).

Shau-Shiun, J. (2010). Vertical guidance performance analysis of the L1-L5 dual-frequency GPS/WAAS user avionics sensor. *Sensors, 10,* 2609-2625. doi:10.3390/s100402609

Shuanggen, J. (2012). *Global navigation satellite systems – Signal, theory and applications.* https://www.intechopen.com/books/623

Simon, J. Ostolaza, J. Moran, J. Fernandez, M. Caro, J., & Madrazo, A. (2012*). On the performance of dual-frequency multi-constellation SBAS: Real data results with operational state-of-the-art SBAS prototype*. Proceedings of the 25th International Technical Meeting of the Satellite Division of the Institute of Navigation ION GNSS.

Speidel, J., Tossaint, M., Wallner, S., & Angelavila-Rodriguez, J. (2013). Integrity for aviation; comparing future concepts. *Inside GNSS, 8*(4), 54-64.

Tabti L., Kahlouche S. & Benadda B. (2018). Improving availability of the EGNOS system in Algeria for dual frequency. *Coordinate Magazine*, 36-40. https://mycoordinates.org/improving-availability-of-the-egnos-system-in-algeria-for-dual-frequency/

Tabti, L., Kahlouche, S., Benadda, B. & Beldjilali, B. (2020). Improvement of a single frequency GPS positioning performance based on EGNOS corrections in Algeria. *Journal of Navigation*. doi.org/10.1017/S037346331900095X.

Tossaint, M., Wallner, S., & Angelavila-Rodriguez, J. (2013). Integrity for aviation; comparing future concepts. *Inside GNSS*. https://insidegnss.com/wp-content/uploads/2018/01/julyaug13-WP.pdf

Vassilev, B., & Vassileva, B. (2010). *Some EGNOS performance results in the context of aircraft navigation*. ELMAR, 2010 proceedings, Zadar, and Croatia.

Walter, T., Blanch, J., & Enge, P. (2010*). Coverage improvement for dual frequency SBAS*. Proceedings of the International Technical Meeting of The Institute of Navigation, San Diego, CA, pp. 344-353.